Facile Preparation of Superhydrophobic Biomimetic Surface Based on Octadecyltrichlorosilane and Silica Nanoparticles

Qingping Ke, Wenqian Fu, Shun Wang, Tiandi Tang,* and Jingfeng Zhang

Department of Chemical Engineering and Processing, College of Chemical and Materials Engineering, WenZhou University, WenZhou, ZheJiang 325000, P. R. China

ABSTRACT The present paper describes the simple and low-cost process for the production of a superhydrophobic surface with micronano hierarchical structure from the chemisorptions of SiO_2 nanoparticles onto polymerized *n*-octadecylsilane. The process was carried out under ambient conditions without the use of expensive equipment. The as-prepared micronano-binary films exhibited a very high contact angle of 179.9° and a low contact hysteresis of 2.5°. On the basis of the results of the characterization techniques, scanning electron microscopy (SEM), Fourier transform infrared spectroscopy (FT-IR) and contact angle (CA) measurements, a formation mechnism of the superhydrophobic micronano structure was proposed. Drop impact experiments on the modified-glass substrate showed that the as-prepared films possess a high-impalement threshold.

KEYWORDS: superhydrophobic • one-step • hierarchical structure • PODS • multilayer • OTS

1. INTRODUCTION

Wettability of a solid surface is an important property, which is determined by its chemical composition as well as its geometry. A surface with an apparent contact angle larger than 150° is generally referred to as superhydrophobic surface. Superhydrophobic surfaces possessing water-repellency and self-cleaning properties have attracted significant recent interest from both academic and industrial research efforts (1−5).

Two strategies are generally adopted for the fabrication of superhydrophobic surfaces: roughening of a hydrophobic surface, and modifying that rough surface with low surface energy materials (6). Much attention has recently been paid to developing approaches to prepare superhydrophobic surfaces (7−10). It is well-known that the combination of a special micronano-binary structure (MNBS) and surface chemistry effects endows the louts-leaf with remarkable water-repellency (11). This inspired us to fabricate superhydrophobic surfaces by mimicking the lotus-leaf MNBS. Alkylsilane polymers are of interest in the fabrication of superhydrophobic surfaces because of their low surface free energy. Superhydrophobic surfaces from alkylsilane-based polymers have been fabricated by silicon etching (12), nanoparticle decoration (13), and Langmuir−Blodgett deposition (14). Xue et al. (15) prepared superhydrophobic films from vinyl-modified silica nanoparticles, which exhibited a high contact angle of 166°. Kulkarni et al. (16) optimized the hydrophobicity of silica particles and obtained a MNBS with contact and sliding angles of 168.2° and <10°, respectively. A one-step fabrication of a superhydrophobic surface based on tetra-ethylorthosilicate and a fluorinated alkyl silane was recently reported (17−19). These works provide a simple and universal method for fabricating superhydrophobic surfaces on many substrates. Dhere et al. (20) reported a more economic process by using an isobutyltrimethoxysilane as a coprecursor, and fabricated water repellent silica films on the glass substrates. However, simple and low-cost methods allowing scale up for industrial applications of the superhydrophobic surfaces are still lacking (21). The current study aimed to find a simple and low-cost process for fabricating superhydrophobic surfaces on large area engineering substrates under ambient conditions. We report a facile preparation of a stable MNBS superhydrophobic surface, which involves self-assembly, polycondensation of octadecylsilane (PODS), and silica nanoparticles chemically bonded onto PODS sheets by hydroxyl shrink. The static angle and contact angle hysteresis of the resultant surface are 179.9 and 2.5°, respectively.

2. MATERIALS AND METHODS

N-Octadecyltrichlorosilane (C_{18}, OTS) (95%) was obtained from Acros. Commercially available glass slides were used as substrates and were first rinsed with deionized water and cleaned by an ultrasonic ethanol bath for 10 min. The cleaned glass was then soaked in Piranha solution for 45 min and rinsed with distilled water. Wilsonart Chemsurf (390# series, from wilsonart) were cleaned by rinsing with ethanol.

SiO_2 nanoparticles (20 mg, 100 nm) and OTS (0.4 mL) were added to ethanol (20 mL). The suspension was dispersed in an ultrasonic cleaner, aged for 30 min, dip-coated on substrates for 1−5 cycles, dried under atmospheric conditions (relatively

* Corresponding author. E-mail: tangtd2006@yahoo.com.cn.
Tel: +86-577-86689366. Fax: +86-577-86689300.
Received for review May 8, 2010 and accepted July 7, 2010
DOI: 10.1021/am1004046

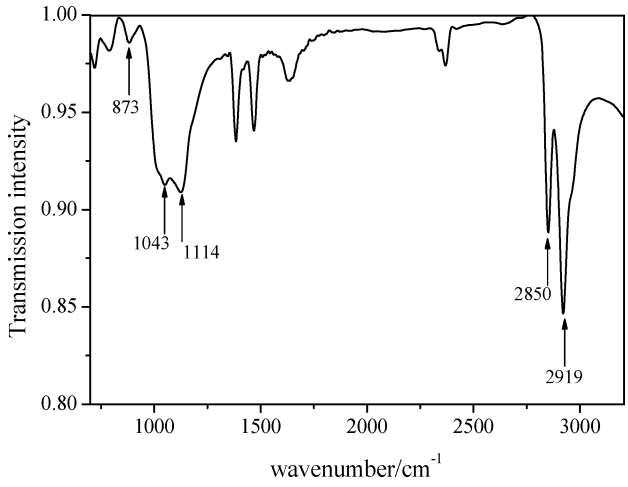

FIGURE 1. IR spectrum of the modified-silica nanoparticles/PODS coating.

humidity 70%, temperature 3.2 °C), and then cured in an oven at 45 °C for 6 h.

The coating layer was removed from the substrates by a surgical blade, and its infrared spectrum was recorded on a Bruker equinox 55 FT-IR spectrometer. The corresponding SEM images of the MNBS were obtained on a JSM 6700F instrument. Static contact angles were measured on a Data Physic measuring system equipped with a CCD camera. Advancing and receding contact angles were measured during the growth and shrinkage of a droplet, respectively. The contact angle values were fitted by the Young−Laplace equation and measured at five different spots for each sample.

3. RESULTS AND DISCUSSIONS

3.1. FT-IR. The modified-silica nanoparticles/PODS coating was obtained as a white layer, and its IR spectrum is shown in Figure 1. The peaks at 2919 and 2850 cm^{-1} correspond to the asymmetric and symmetric stretching CH_2 groups, respectively. The peak at 873 cm^{-1} was assigned to the Si−OH stretching vibration, and the peaks at 1000−1300 cm^{-1} were assigned to the Si−O−Si stretching vibration (22). This indicated that the hydrolysis of OTS occurred but the polycondensation of $RSi(OH)_3$ was incomplete.

3.2. Surface Morphology and Wettability. Figure 2a is a low-magnification SEM image showing the film's surface morphology as "flowerlike" microstructures. Figure 2b is a higher-magnification view showing that the leaves of the flowers have a uniform length of about 5 μm, on which nano-SiO_2 particles were observed (Figure 2b insert). These results indicated a MNBS structure had been formed on the glass surface.

To ensure adequate coverage of the substrate coating was achieved, it was necessary to perform 2−4 dip-coating cycles. The wettability of the as-prepared MNBS was studied as a function of coverage by increasing the number of dip-coating cycles. As shown in Figure 3, one cycle resulted in a contact angle of 148.2°. The contact angle increased to 179.6° upon the addition of a second cycle. Zhao et al. (23) fabricated a superhydrophobic MNBS coating in one-step procedure by casting a solution of bisphenol A polycarbonate in the presence of moisture. However, controlled relative humidity was required during the vapor-induced phase

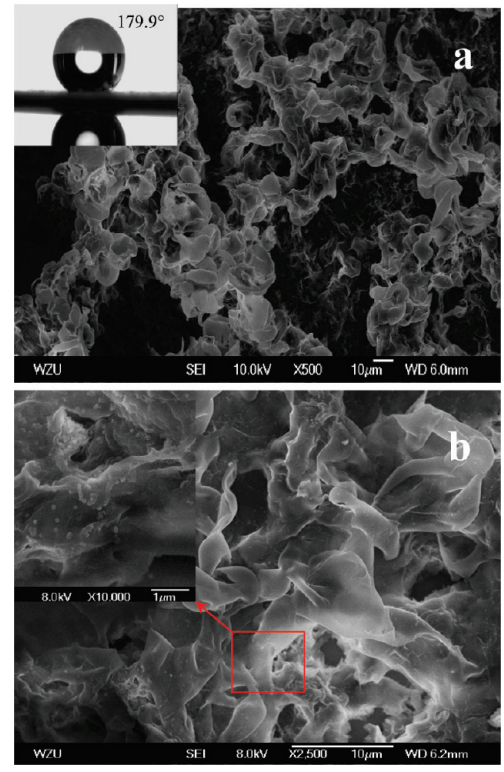

FIGURE 2. SEM images and wettability of the PODS-SiO_2 nanocomposite surface. The water droplet volume was 5 μL.

separation. Luo et al. (24) also prepared a superhydrophobic MNBS by spraying the polytetrafluoroethylene (PTFE) precursors on stainless steel. Compared to these reports, a more energy- and cost-efficient process is presented in the current study.

The reason for the increase in contact angle is thought to be that the increasing the dip-coating cycles may augment the roughness factor by enhancing surface coverage, as shown in the SEM images of Figure 3. According to Wenzel's (25) and Cassie−Baxter's laws (26), roughness and porous structures enhance both hydrophobicity and hydrophilicity depending on the nature of the corresponding flat surface. In this study, one cycle was not enough to form a superhydrophobic surface, and further dip-coating cycles were required. After four dip-coating cycles, the resultant water contact angle of the PODS-SiO_2 coated films was 179.9° (inset, Figure 2a), and contact angle hysteresis was 2.5° (advancing contact angle/receding contact angle = 157.3°/154.8°). It was found that after water droplet deposited on the PODS-SiO_2 surface for about 3 min, the contact angle for one and two cycles decreased from 148.2 to 145.1° and 179.6 to 158.9°, respectively (Figure 4). When the number of dip-coating cycles exceeded three, the deposited water droplet entered a stable suspended state and the contact angle was constant and independent of deposition time. Generally, water droplets cannot easily roll off the surface as they are strongly pinned in the Wenzel state (27), which leads to a high contact angle hysteresis and large sliding angle. Conversely, in a Cassie state, water droplets may slide off the surface at a small tilt angle. It has been shown that on some artificial superhydrophobic surfaces there exists a

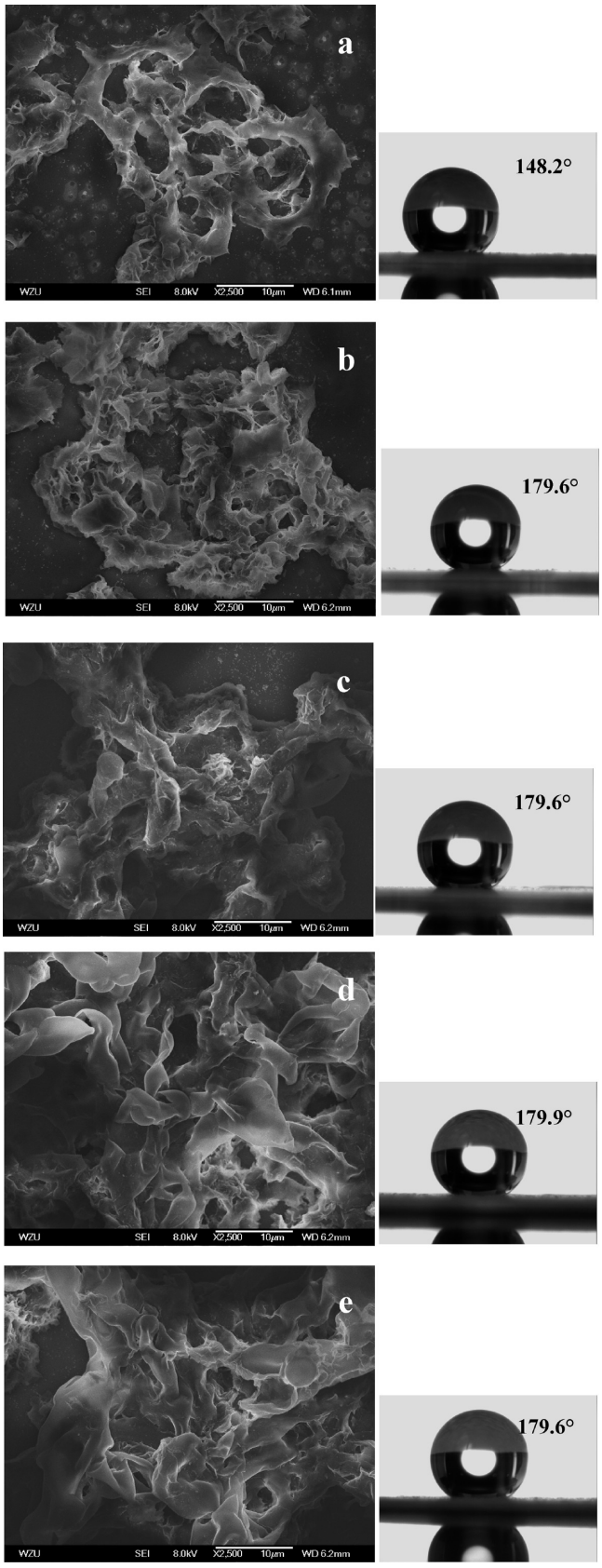

FIGURE 3. Surface morphology and wettability dependence of the as-prepared MNBS on the number of dip-coating cycles: (a) 1, (b) 2, (c) 3, (d) 4, (e) 5.

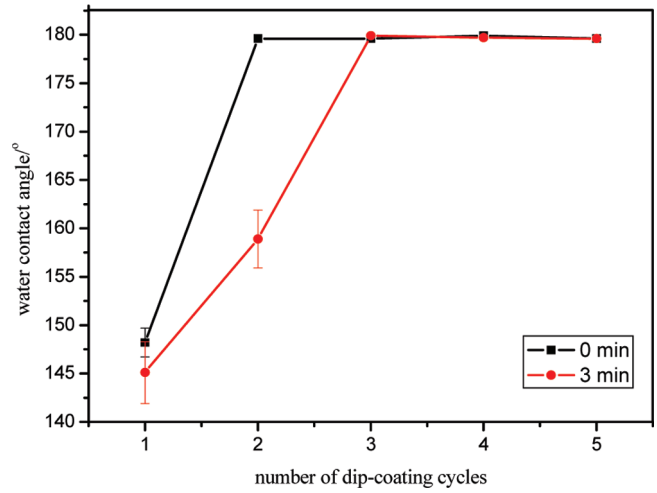

FIGURE 4. Dependence of contact angle on the number of dip-coating cycles. The concentration of SiO_2 and OTS is 1 mg/mL and 2% (v/v) in the ethanol, respectively. Water deposited on PODS-SiO_2 surface for 0 and 3 min. "0 min deposition" means that the measurement of the contact angle just after deposition. Error bars represent the standard error of the mean for each value of the measurement contact angle.

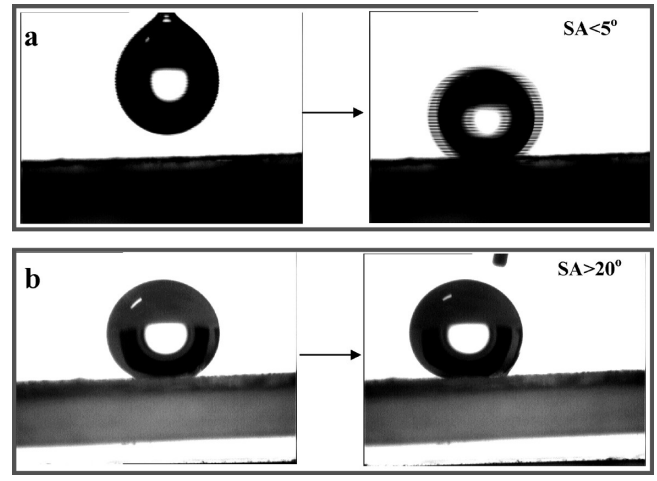

FIGURE 5. Sliding behavior of the PODS-SiO_2 surface with two cycles of dip coating: (a) drops on the PODS-SiO_2 surface at a tilt angle of 5°; (b) drops on the PODS-SiO_2 surface at the horizontal position which was then tilted >20° after 3 min. SA means sliding angle.

metastable Cassie state. For those surfaces, a transition from the metastable Cassie to Wenzel states could be induced by applying mechanical pressure, dropping from some height, or even the force exerted by the weight of the drop itself (27, 28). In our study, the variation of contact angle for one to two dip-coating cycles may be explained as follows. The water droplet could be exist at metastable Cassie state when a 5 μL droplet was gently brought into contact with the rough PODS-SiO_2 surface it rolled off (Figure 5a, the rough surface with a tilt angle of 5°). A transition from the metastable Cassie to Wenzel states may occur under the effect of the droplet weigh, which decreased the contact angle and lead to loss of its sliding behavior on the PODS-SiO_2 surface (Figure 5b).

3.3. Formation Mechanism. The preparation of surfaces with a MNBS has been reported by various methods (29−35), including coating colloidal material on micropillars, decorating carbon nanotubes with microspheres. Tedious

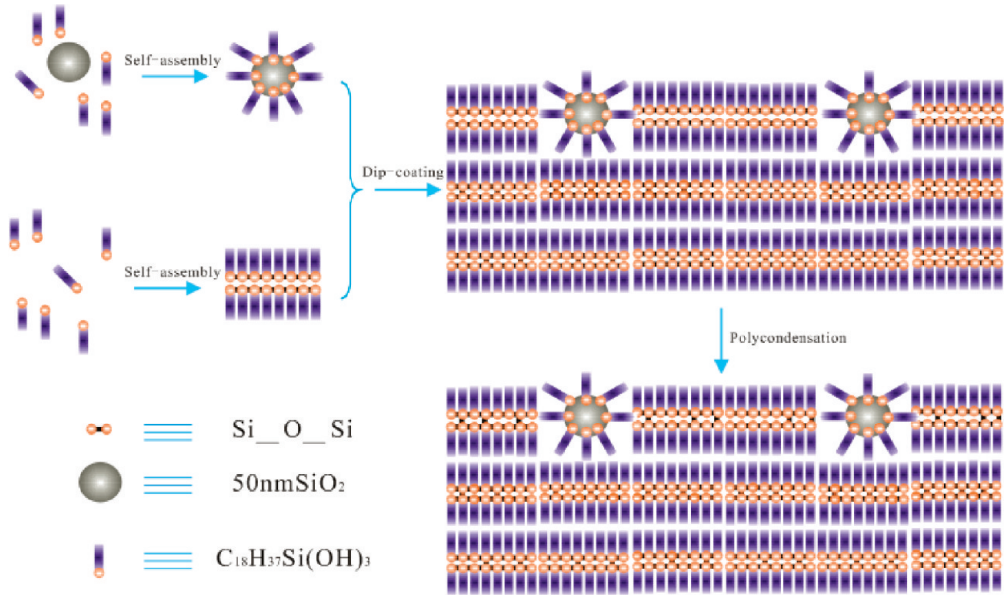

FIGURE 6. Schematic illustration of the formation process of the PODS-SiO_2 hierarchical structure.

experimental steps and expensive equipment are generally required for these procedures. In our previous work (22), a superhydrophobic surface was created by self-assembling ODS on the glass, and subsequently forming PODS nanosheets via solvent extraction. In the current study, we have demonstrated a one-step route to fabricate a hierarchical superhydrophobic structure via a solution immersion process, and this is an economic process for the practical application of superhydrophobic MNBS. A possible formation mechanism of the superhydrophobic MNBS was proposed as follows (Figure 6): An ODS self-assembled monolayer (SAM) was first grown on SiO_2. During this stage, ODS also self-assembled to form an ODS bilayer. The ODS bilayer and modified-SiO_2 were dip-coated onto the glass surface with a resulting highly orderly structure from the coeffect of solvent/water. Third, the ODS bilayer partly polymerized to PODS and a chemical reaction occurred between PODS and the modified-SiO_2.

3.4. On the Surface Modification of Engineering Materials and Its Mechanical Resistance. According to the proposed superhydrophobic PODS-SiO_2 formation mechanism, the interaction between the glass substrate and coating materials should have no detrimental effect on superhydrophobicity, thus superhydrophobic surfaces could presumably be obtained on different substrates. The thickness of the coating layer could be easily controlled by varying the number of dip-coating cycles. Thus, the Wilsonart Chemsurf substrate was used for surface modification experiments. Optical images of water beading on this substrate are shown in Figure 7. Compared to the hydrophilicity of unmodified Wilsonart Chemsurf (Figure 7, black box), the modified substrate exhibited far higher water-repellency. The red droplets slid off the modified substrate and left no trace (from Figure 7a to Figure 7b). This shows that our method can be used to create large-scale superhydrophobic coatings.

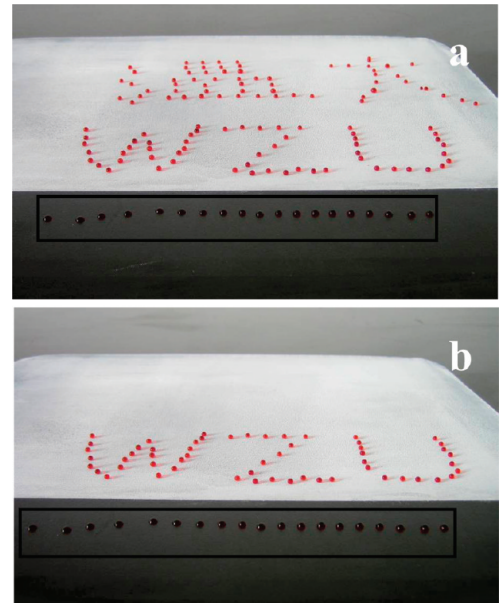

FIGURE 7. Optical images of water beading on Wilsonart Chemsurf substrate treated with and without PODS-SiO_2 MNBS nanocomposite, the zone of water beads deposited inside the black box without modifying by PODS-SiO_2 MNBS nanocomposite: (a) containing the Chinese characters consisting of water droplets; (b) the Chinese characters have rolled off the surface.

The methods of evaluating the mechanical resistance of superhydrophobic surfaces have been discussed though the drop impact and shear processes (36, 37). To engineer the PODS-SiO_2 surface for practical applications, such as aircraft engines or heat exchangers, one must consider the surface wettability under dynamic conditions. In this study, the mechanical resistance of the PODS-SiO_2 surface was studied by drop impact experiments. Figure 8 shows the snapshots of 6 μL water drops free-falling on the superhydrophobic PODS-SiO_2 surface with a tilt angle of ~5°. The physical property of the drops is the following: fluid density ρ=1100 kg/m^3, drops diameter $d = 2.30 \pm 0.07$ mm, surface tension

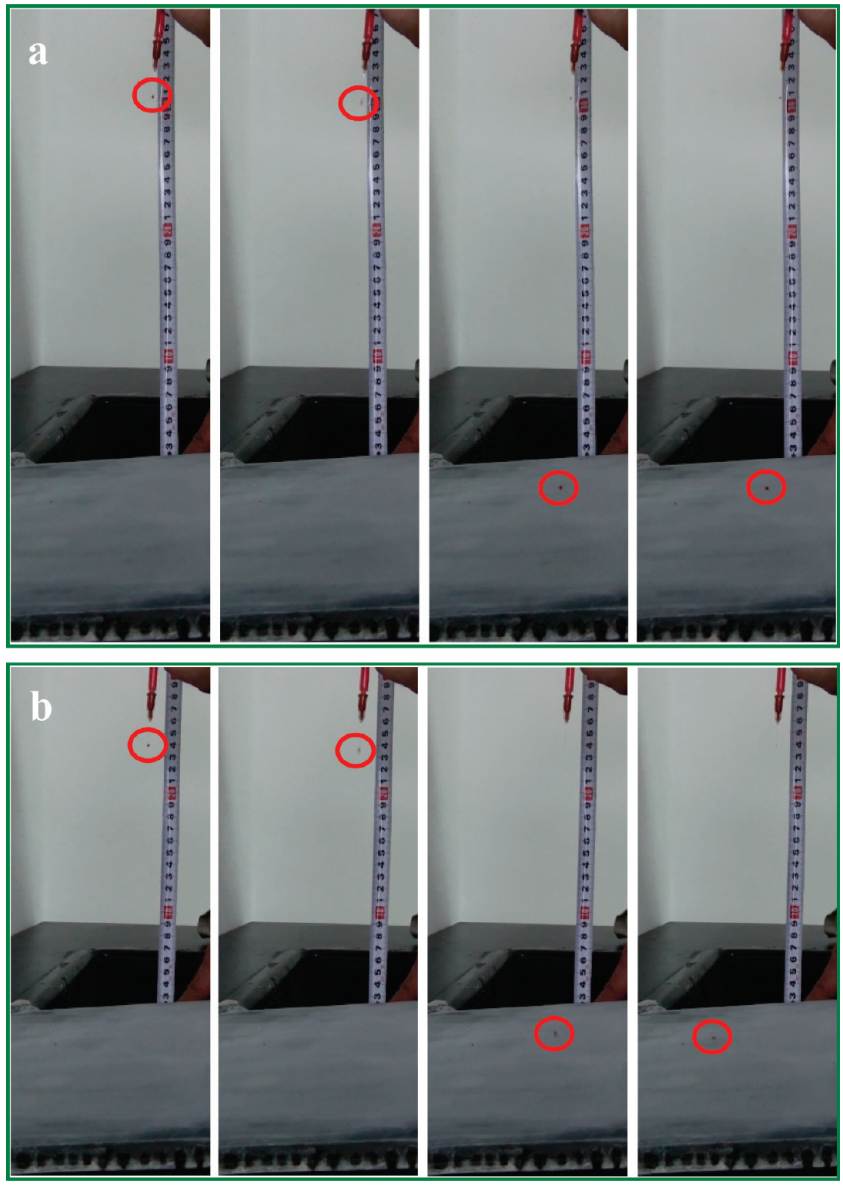

FIGURE 8. Snapshots of 6 μL water drops free-falling on the superhydrophobic PODS-SiO_2 surface with a tilt angle of ~5°: (a) Weber number = 208; (b) Weber number = 186.

σ =0.066 N/m. The drops impact with the PODS-SiO_2 surface with a velocity of V=2.36 m/s and the corresponding Weber number ($W = \rho V^2 d/\sigma$) is 208 (Figure 8a). In this case, the drop cannot roll off the PODS-SiO_2 surface. When $W <$ 208, the droplet could slid off the PODS-SiO_2 surface completely (the pressure of the drops impact on the PODS-SiO_2 surface was 6 KPa, Figure 8b).

4. CONCLUSION AND OUTLOOK

A superhydrophobic MNBS surface with high contact angle and low contact angle hysteresis has been obtained by a one-step preparation. The facile method is of low cost and is applicable to a variety of surfaces. The formation process of the MNBS surface was described as the hydrolysis of OTS, subsequent intermolecular self-assembly, self-assembly monolayer formation on SiO_2, and the slow polycondensation of ODS and modified-SiO_2. Potential applications of this approach to membrane distillation processes, heat transfer, and oil−water separation process are anticipated.

Acknowledgment. This work was supported by the Natural Science Foundation of Zhejiang Province of China (Y4090084) and the Science and Technology Program of WenZhou (G20080144).

REFERENCES AND NOTES

(1) Furmidge, C. G. L. *J. Colloid Sci.* **1962**, *17*, 309–324.
(2) Pastine, S. J.; Okawa, D.; Kessler, B.; Rolandi, M.; Llorente, M.; Zettl, A.; Frechet, J. M. J. *J. Am. Chem. Soc.* **2008**, *130*, 4238–4239.
(3) Yagai, S.; Ishii, M.; Karatsu, T.; Kitamura, A. *Angew. Chem., Int. Ed.* **2007**, *46*, 8005–8009.
(4) Tuteja, A.; Choi, W.; Ma, M.; Mabry, J. M.; Mazzella, S. A.; Rutledge, G. C.; Mckinley, G. H.; Cohen, R. E. *Science* **2008**, *318*, 1617–1622.
(5) Wang, C. X.; Yao, T. J.; Wu, J.; Ma, C.; Fan, Z. X.; Wang, Z. Y.; Cheng, Y. R.; Lin, Q.; Yang, B. *ACS Appl. Mater. Interfaces* **2009**, *1*, 2613–2617.
(6) (a) Nakanishi, T.; Shen, Y. F.; Wang, J. B.; Li, H. G.; Fernandes, P.; Yoshida, K.; Yagai, S.; Takeuchi, M.; Ariga, K.; Kurth, D. G.;

Möhwald, H. *J. Mater. Chem.* **2010**, *20*, 1253–1260. (b) Li, X. M.; Reinhoudt, D.; Crego-Calama, M. *Chem. Soc. Rev.* **2007**, *36*, 1350–1368. (c) Crick, C. R.; Parkin, I. P. *J. Mater. Chem.* **2009**, *19*, 1074–1076. (d) Zhang, X.; Shi, F.; Niu, J.; Jiang, Y.; Wang, Z. *J. Mater. Chem.* **2008**, *18*, 621.
(7) Zhao, N.; Xu, J.; Xie, Q.; Weng, L.; Guo, X.; Zhang, X.; Shi, L. *Macro. Rapid Comm.* **2005**, *26*, 1075–1080.
(8) Zhang, L.; Li, Y.; Sun, J.; Shen, J. *J. Colloid Interface Sci.* **2008**, *319*, 302–308.
(9) Gao, L. C.; McCarthy, T. J. *Langmuir* **2008**, *24*, 362–364.
(10) Yang, S.; Chen, S.; Tian, Y.; Feng, C.; Chen, L. *Chem. Mater.* **2008**, *20*, 1233–1235.
(11) (a) Barthlott, W.; Neinhuis, C. *Planta* **1997**, *202*, 1. (b) Sun, T.; Feng, L.; Gao, X.; Jiang, L. *Acc. Chem. Res.* **2005**, *38*, 644–652. (c) Lee, W.; Jin, M.; Yoo, W.; Lee, J. *Langmuir* **2004**, *20*, 7665.
(12) (a) Cao, L. L.; Hu, H. H.; Gao, D. *Langmuir* **2007**, *23*, 4310–4314. (b) Cao, M. W.; Song, X. Y.; Zhai, J.; Wang, J. B.; Wang, Y. L. *J. Phys. Chem. B* **2006**, *110*, 13072–13075. (c) Xiu, Y. H.; Zhu, L. B.; Hess, D. W.; Wong, C. P. *Nano Lett.* **2007**, *7*, 3388–3393. (d) Wang, M. F.; Raghunathan, N.; Ziaie, B. *Langmuir* **2007**, *23*, 2300–2303.
(13) Zhai, L.; Cebeci, F. C.; Cohen, R. E.; Rubner, M. F. *Nano Lett.* **2004**, *4*, 1349–1353.
(14) (a) Hsieh, C. T.; Chen, W. Y.; Wu, F. L.; Hung, W. M. *Diamond Relat. Mater.* **2010**, *19*, 26–30. (b) Wu, D.; Chen, Q. D.; Xia, H.; Jiao, J.; Xu, B. B.; Lin, X. F.; Xu, Y.; Sun, H. B. *Soft Matter* **2010**, *6*, 263–267. (c) Yao, T. J.; Wang, C. X.; Lin, Q.; Li, X.; Chen, X. L.; Wu, J.; Zhang, J. H.; Yu, K.; Yang, B. *Nanotechnology* **2009**, *20*, 065304. Tsai, P. S.; Yang, Y. M.; Lee, Y. L. *Langmuir* **2006**, *22*, 5660–5665.
(15) Xue, L. J.; Li, J.; Fu, J.; Han, Y. C. *Colloids Surf. A* **2009**, *338*, 15–19.
(16) Kulkarni, S. A.; Ogale, S. B.; Vijayamohanan, K. P. *J. Colloid Interface Sci.* **2008**, *318*, 372–379.
(17) Sheen, Y. C.; Huang, Y. C.; Liao, C. S.; Chou, H. Y.; Chang, F. C. *J. Polym. Sci., Part B: Polym. Phys.* **2008**, *46*, 1984–1990.
(18) Wang, H. X.; Fang, J.; Chang, T.; Ding, J.; Qu, L. T.; Dai, L. M.; Wang, X. G.; Lin, T. *Chem. Commun.* **2008**, 877–879.
(19) Darmanin, T.; Guittard, F. *J. Am. Chem. Soc.* **2009**, *131*, 7928–7933.
(20) Dhere, S. L.; Latthe, S. S.; Kappenstein, C.; Pajonk, G. M.; Ganesan, V.; Rao, A. V.; Waghe, P. B.; Gupta, S. C. *Appl. Surf. Sci.* **2010**, *256*, 3624–3629.
(21) Yang, H.; Pi, P. H.; Cai, Z. Q.; Wen, X. F.; Wang, X. B.; Cheng, J.; Yang, Z. R. *Appl. Surf. Sci.* **2010**, *256*, 4095–4102.
(22) Ke, Q. P.; Li, G. L.; Liu, Y.; He, T.; Li, X. M. *Langmuir* **2010**, *26*, 3579–3584.
(23) Zhao, N.; Xu, J.; Xie, Q. D.; Weng, L. H.; Guo, X. L.; Zhang, X. L.; Shi, L. H. *Macro. Rapid Commun.* **2005**, *26*, 1075–1080.
(24) Luo, Z. Z.; Zhang, Z. Z.; Wang, W. J.; Liu, W. M.; Xue, Q. J. *Mater. Chem. Phys.* **2010**, *119*, 40–47.
(25) Wenzel, R. N. *Ind. Eng. Chem.* **1936**, *28*, 988–994.
(26) Cassie, A. B. D.; Baxter, S. *Trans. Faraday Soc.* **1949**, *40*, 546–551.
(27) Brunet, P.; Lapierre, F.; Thomy, V.; Coffinier, Y.; Boukherroub, R. *Langmuir* **2008**, *24*, 11203–11208.
(28) Lafuma, A.; Quere, D. *Nat. Mater.* **2003**, *2*, 457–460.
(29) Camarota, B.; Mann, S.; Onida, B.; Garrone, E. *ChemPhysChem* **2007**, *8*, 2363–2366.
(30) Mao, C.; Liang, C. X.; Luo, W. P.; Bao, J. C.; Shen, J.; Hou, X. M.; Zhao, W. B. *J. Mater. Chem.* **2009**, *19*, 9025–9029.
(31) Li, X. M.; He, T.; Crego-Calama, Reinhoudt, M.; D. N. *Langmuir* **2008**, *24*, 8008–8012.
(32) Hu, X. G.; Dong, S. J. *J. Mater. Chem.* **2008**, *18*, 1279–1295.
(33) Bae, G. Y. B.; Min, G.; Jeong, Y. G.; Lee, S. C.; Jang, J. H.; Koo, G. H. *J. Colloid Interface Sci.* **2009**, *337*, 170–175.
(34) Liu, X.; He, J. *J. Colloid Interface Sci.* **2007**, *314*, 341–345.
(35) Li, M.; Xu, J. H.; Lu, Q. H. *J. Mater. Chem.* **2007**, *17*, 4772–4776.
(36) Merlen, A.; Brunet, P. *J. Bionic Eng.* **2009**, *6*, 330–334.
(37) Xiu, Y. H.; Liu, Y.; Hess, D. W.; Wong, P. C. *Nanotechnology* **2010**, 155705.

AM1004046